Electrochemical Investigation of Magnesium-doped Copper Ferrite Nanostructures for asymmetric type supercapacitor application

M. Selvakumar [a,b], S. Maruthamuthu [b]*, E. Vijayakumar[c], B. Saravanakumar [d]

A. Tony Dhiwahar [e]

[a.] *Physics Division, Forensic Sciences department, Chennai - 600 004, Tamil Nadu, India*

[b.] *PSG Institute of Technology and Applied Research Coimbatore - 641 062, Tamil Nadu, India*

[c.] *Department of Materials Science and Engineering, Korea University,Korea*

[d.] *Dr. Mahalingam College of Engineering and Technology, Pollachi - 642 003, Tamil Nadu, India*

[e.] *Nehru Arts and Science College, Coimbatore - 641 105, Tamil Nadu, India*

Corresponding author: * smaruthamuthu@gmail.com (S. Maruthamuthu)

ABSTRACT

In this present study, the synthesis of magnesium-doped copper ferrite namely $Cu_xMg_{1-x}Fe_2O_4$ (x=1, 0.9, 0.7 and 0.5) through a facile microwave route has been reported. Furthermore, cubic crystalline structure, functional group and nanostructured materials of the same have been discussed. The electrochemical studies of magnesium-doped copper ferrite (MCF) have been done by assembling a three-electrode conventional electrochemical cell with MCF samples as working electrode, a platinum wire as counter electrode, a silver (Ag)/silver chloride (AgCl) as reference electrode and 2 M KOH aqueous solution as electrolyte. The study of electrochemical performance of Mg-doped and undoped copper ferrite electrode reveals that they show battery-type behaviour with the transfer of two electrons (Mg to Mg^{2+}) in 2 M KOH electrolyte in the potential window 0.45 to 0.35 V. Further, un-oxidized MgO oxidizes leading to quasi-conversion reaction. Additionally, the electrode (MCF) exhibits a greater specific capacity of 737.5 F g^{-1} at 1 A g^{-1}. It has been found that the MCF3 electrode holds 70 % of initial capacitance, which is higher than the CF electrode (33%) after 4000 continuous galvanostatic charge/discharge (GCD) cycles. An asymmetric type of supercapacitor cell has been fabricated using MCF as the positive electrode, activated carbon (AC) as the negative electrode, 2 M KOH as the electrolyte and polypropylene as the separator. The fabricated (MCF\\AC) supercapacitor has yielded maximum specific energy of 62.61 W h kg^{-1} at a specific power of 1168 W kg^{-1}. These electrochemical features suggest that MCF could be a feasible material for developing supercapacitor electrodes.

Keywords: Microwave combustion process, copper ferrite, asymmetric type supercapacitor, IR drop, electrochemical features

Introduction:

Tunable nanostructured materials with low-cost and rapid processing have various practical applications in the modern electronic era, but now-a-days, increase in the usage of electrical and electronic gadgets, and home appliances in the fast-growing world results in energy and power deficiency. In the last century, combustion of fossil fuels such as coal, wood, lignite, oil and so on were used as energy source which contaminate our healthy environment. Henceforth energy source and energy storage device are significant for the development and improvement of the society and the environment. Hence, they play a vital role in order to protect and save the environment. In this aspect, supercapacitors are the most expected devices which are desirable, due to their salient features, namely swift charging, slow discharging rate, superior power density and prolonged life time [1-5]. Hence supercapacitors have been identified as a research hotspot for many research groups to the progression of energy-storage devices.

Primarily, in supercapacitors, materials such as conducting polymers and metal oxides are being used to fabricate a pioneer class of electrode materials. When the electrode is made up of conducting polymer, swelling and deterioration may turn up in the conducting polymer at the time of intercalation and de-intercalation leading to poor cyclic stability. Henceforth, research groups take diversion towards metal oxides, especially in the form of nanostructured ferrites in order to fabricate electrodes which are employed in supercapacitors. Ferrites have a couple of diverse crystal structure; specific regular spinel and inverse spinel by blending of iron oxides and metal oxides [6]. The spinel ferrite structure can be expressed in the form of equation such as $Y^{2+}Fe^{3+}O_4^{2-}$ [Y=Mg^{2+}, Ca^{2+}, Fe^{2+}, Ni^{2+}, Cu^{2+}, Zn^{2+}, and so on]. Regular spinel consists of two different spots referred to as A and B. Spot A is tetrahedral site in which metal having a valency of two is enveloped by four oxygen ions, whereas spot B is octahedral in which metal having a valency of three is confined by six oxygen ions (O^{2-}). Many metal oxides are there in which copper ferrite is picked up as the desirable material for fabricating electrode in supercapacitors due to its amazing benefits like good availability, cost effectiveness, harmlessness and its crystal structure, especially the spinel structure. Nevertheless, lack of cyclic stability, poor kinetics, and short fall of electrical conductivity have restricted the use of copper ferrite in commercial applications. In order to

overcome these glitches, CF is fused with Mg instead of copper in order to design promising electrode material to get enhanced supercapacitive behavior. Furthermore, the regular spinel crystal structure could be altered from normal to inverted spinel by altering copper ferrite with Mg ions. Particularly, as the percentage of chemical compositions and position of the parent atoms in copper ferrite are altered, the structural, optical, magnetic, electrical and chemical properties could be enriched.

Monika Saini et al. designed and synthesized PANI/$Mg_{0.6}Cu_{0.4}Fe_2O_4$ nanocomposites through *in situ* chemical oxidation polymerization method. The nanocomposites showed shielding effectiveness value up to 32.8 dB in the X-band frequency range [7]. M.A. Dar et al. employed sol-gel route to synthesize magnesium substituted nickel-copper-zinc nano-ferrite (Ni–Cu–Zn ferrite) for the development of magnetic properties and reported that the coercivity was diminished with the inclusion of Mg, which would be helpful for power applications [8]. M.A. Ahmed et al. studied the variation on structural and magnetic properties of copper ferrite due to the addition of Mg^{2+} in copper ferrite prepared by different routes namely standard ceramic method, co-precipitation method, citrate method and sol–gel method [9]. M.A. Gabal et al. synthesized nanocrystalline Mg-substituted NiCuZn ferrites successfully, for the first time, with the help of metal nitrates and newly extracted egg white. The greatest saturation magnetization has been found to be in the composition Ni0.3Cu0.2Zn0.3 $Mg_{0.2}Fe_2O_4$ [10]. Yuan Zhou et al. prepared $Li_xCu_{0.6}Mg_{0.4-x}Fe_2O_4$ (x=0, 0.1, 0.2, and 0.3) by calcining predecessor oxalates in air to establish the specific saturation magnetizations (M_s) and coercivity (H_c) [11]. U. Wongpratat et al. fabricated $Ni_{1-x}Mg_xFe_2O_4$ nanoparticles by a wet chemical method for supercapacitor behavior and showed that specific capacitances were as high as 259.89 F/g and 133.95 F/g after the promising electrode performances were examined for $MgFe_2O_4$ and $Ni_{0.25}Mg_{0.75}Fe_2O_4$ electrodes, respectively [12]. M.K. Shobana et al. prepared magnesium-doped Ni ferrite nanoparticle ($Ni_{1-x}Mg_xFe_2O_4$) and confirmed as an anode material for Li ion batteries with great reversible capabilities for the Mg doped Ni ferrite nanoparticle electrodes [13]. M. Kaur et al. reported encouraging magnetic and micro structural properties of $Mg_{0.6}Cd_{0.4}Fe_2O_4$ nanomaterials indicating their potential as soft magnetic materials [14]. H M Zaki et al. prepared nano-crystalline $Mg_{0.5}Cu_xZn_{0.5-x}Fe_2O_4$ ($0 \leq x \leq 1.0$) ferrite powders using co-precipitation route and magnetic data displayed that the saturation magnetization (M_s) rises with Cu^{2+} concentration up to x = 0.2 and then decreases with further increase of Cu^{2+} ions in this ferrite system [15]. N. Varalaxmi et al.

have reported the synthesis of Mg-substituted NiCuZn ferrites by conventional double ceramic techniques to study the dielectric behavior of the synthesized series of ferrites [16].

From the above discussion it has been found in the literature, Mg doped ferrites have been studied extensively for their magnetic and dielectric properties only. In the present study, a new attempt has been made to synthesis magnesium doped $CuFe_2O_4$ and study the electrochemical properties. In this regard, anode materials ($Cu_xMg_{1-x}Fe_2O_4$ X=1, 0.9, 0.7, and 0.5) have been synthesized by microwave combustion process with L-arginine as fuel at 500°C and the physical and chemical parameters of the materials/samples have been measured with the help of XRD, FT-IR and SEM with EDX. The anode candidate made of Mg/$CuFe_2O_4$/Carbon black and polytetrafluoroethylene (binders) has been analysed in basic medium (2 M KOH). Current-Voltage curve, Voltage-Time curve, percentage of retaining of capacitance, specific capacitance and impedance of bare copper ferrite and Mg-doped copper ferrite have been studied with the aid of cyclic voltammetry (CV) and discussed. An asymmetric supercapacitor with twin electrode device using Mg-doped copper ferrite and higher surface area activated carbon (AC) has been assembled. The present work finds that inclusion of Mg in $CuFe_2O_4$ considerably improves the supercapacitive features of the doped composite material in terms of capacitance, rate of performance, and cyclic stability than the bare $CuFe_2O_4$ sample in 2M KOH electrolyte.

2. Experimental Work

2.1 Synthesis of CF and MCF nanostructure:

Using simplistic microwave combustion technique, a set of CF and MCF nanoparticles ($Cu_xMg_{1-x}Fe_2O_4$ in the ratio of 1, 0.9, 0.7 and 0.5) was synthesized with the aid of AR grade high purity (99%) chemical reagents of magnesium nitrate (Mg $(NO_3)_2.6H_2O$), ferric nitrate ($Fe(NO_3)_3.9H_2O$, nickel nitrate ($Ni(NO_3)_2$) and L-arginine ($C_6H_{14}N_4O_2$) acquired from Merck, India. Moreover, the ratio between the fuel and the oxidizer was maintained to be unity in order to release the maximum energy in the reaction [fuel (U)/oxidizer (N) =1]. Hence, appropriate weights of (Mg $(NO_3)_2.6H_2O$) and (Cu $(NO_3)_2.3H_2O$), 0.808 g of (Fe $(NO_3)_3.9H_2O$, and 0.266 g of $C_6H_{14}N_4O_2$ were taken in the form of fuel. They were dissolved in 50 mL of double distilled water and magnetically stirred nearly for an hour. Utmost care was taken in order to transfer the solution to a 150-mL crucible made up of silica. In the combustion process, the solution was kept in a microwave oven used at home (800 W, CE1041DFB/XTL, and 2.54 GHz frequency) for 10

min. Once the combustion process was completed, the samples were removed from the microwave oven and maintained at 500°C for 2 h, which resulted in the nanoparticles of $Cu_{0.9}Mg_{0.1}Fe_2O_4$ named as MCF1. By changing the concentration of (Mg $(NO_3)_2.6H_2O$) and (Cu $(NO_3)_2.3H_2O$), $Cu_{0.7}Mg_{0.3}Fe_2O_4$, $Cu_{0.5}Mg_{0.5}Fe_2O_4$ were synthesized and named as MCF3 and MCF5 respectively. The same procedure was implemented without using Mg source in order to prepare the bare nanoparticle of ferrite named as CF.

2.2 Analytical instruments used

With the help of a RIGAKU (Japan make) powder X-ray diffractometer, the crystallinity and the size of CF and MCFs nanoparticle samples were examined using the wavelength of X-ray of 1.5418 Å (CuKα) between 2θ ranges from 20° to 80°. The FTIR spectra of CF and MCF nanoparticle samples were recorded with the aid of a Nicolet iS10 spectrometer. Using a JEOL (model No. 6360) high-resolution Scanning Electron Microscope (SEM) system embedded with Energy Dispersive X-ray analysis (EDX), the surface morphological investigations of manufactured CF and MCF nanoparticle were carried out.

2.3. Electrode preparation for electrochemical analysis

A CHI 660C (CH Instruments Inc., USA) electrochemical workstation was used to perform all the electrochemical measurements, which is a three-electrode setup. In general, the working electrode was made up of 85 wt. % of the synthesized samples CF/MCF, 10 wt. % carbon black i.e., Super-P, and 5 wt. % binding material such as polytetrafluoroethylene (PTFE). The working electrodes were made up of synthesised samples, as usual a platinum wire was employed as counter electrode and a silver (Ag)/silver chloride (AgCl) served as the reference electrode. The slurry was prepared with the help of ethanol. The surface of the current collector made up of nickel foam of (1 cm^2) has been solidly coated with the mixture of the above-mentioned slurry. Before coating the active materials, Ni foam current collectors were cleaned up using 37 Wt % of HCl to remove the dirt present on the exterior boundary of the materials and kept at 60°C for 2 h to get free from the moisture. Furthermore, the Ni foam was also cleaned with the aid of both ethanol and double-distilled water. Using cyclic voltammetry, the charge-discharge measurements, and impedance measurements were then examined for the prepared electrodes in 2 M KOH liquid electrolyte.

Finally, the supercapacitive features were calculated for the active electrode with the mass of 0.8 mg.

2.4. Design of asymmetric type supercapacitor device

An asymmetric type of supercapacitor device was patched in a sandwich model using MCF3 as a positive electrode, activated carbon bought from Sigma-Aldrich with the dimension of 1100 m^2/g as a negative electrode, and a partition made by polypropylene sheet in 2 M KOH electrolyte medium. During the charging-discharging cycles, the charge was blanched through balancing the mass such that $(m_+/m_-) = (C_-V_-)/(C_+V_+)$, where, m_+, and m_- are mass (mg) of the fabricated electrode made of MCF (anode) and AC (cathode), C_- and C_+ are the specific capacitances (F g^{-1}) estimated at the same scanning rate, V is the active potential aperture (V) between MCF and AC electrodes. The comprehensive mass of the electrodes is taken as 1.2 mg such that $m_+ = 2\ m_-$ i.e., 0.8 mg of MCF and 0.4 mg of AC in order to balance the mass in the fabricated supercapacitor device. In this study, the potential window is narrowed down between 0 and 1 V because aqueous KOH electrolyte is prone to be extremely susceptible to oxygen evolution reaction beyond 1V.

The prominent feature of supercapacitor is the gravimetric/specific capacitance (C_S) measured in terms of Fg^{-1} with respect to charging and discharging contour of active material in the electrode is assessed using the following relation.

$$C_s = \frac{I * dt}{m * dv} \text{----------(1)}$$

where C_s - specific capacitance (F g^{-1}), *I/m* - current density (A g^{-1}), *dt* - discharge time (s), and *dv* potential aperture (voltage)

The following equations are used to govern the energy and power density of fabricated asymmetric supercapacitor

$$E = \frac{1}{2*3.6} C_S * (\Delta V)^2 \text{----------(2)}$$

$$P = \frac{E}{t} * 3600 \text{----------(3)}$$

where *E* - energy density (W h kg^{-1}), *P* - power density (W kg^{-1}) and t - time of discharge (s).

3.0 Results and discussion

3.1 Structural, morphological and surface area analysis

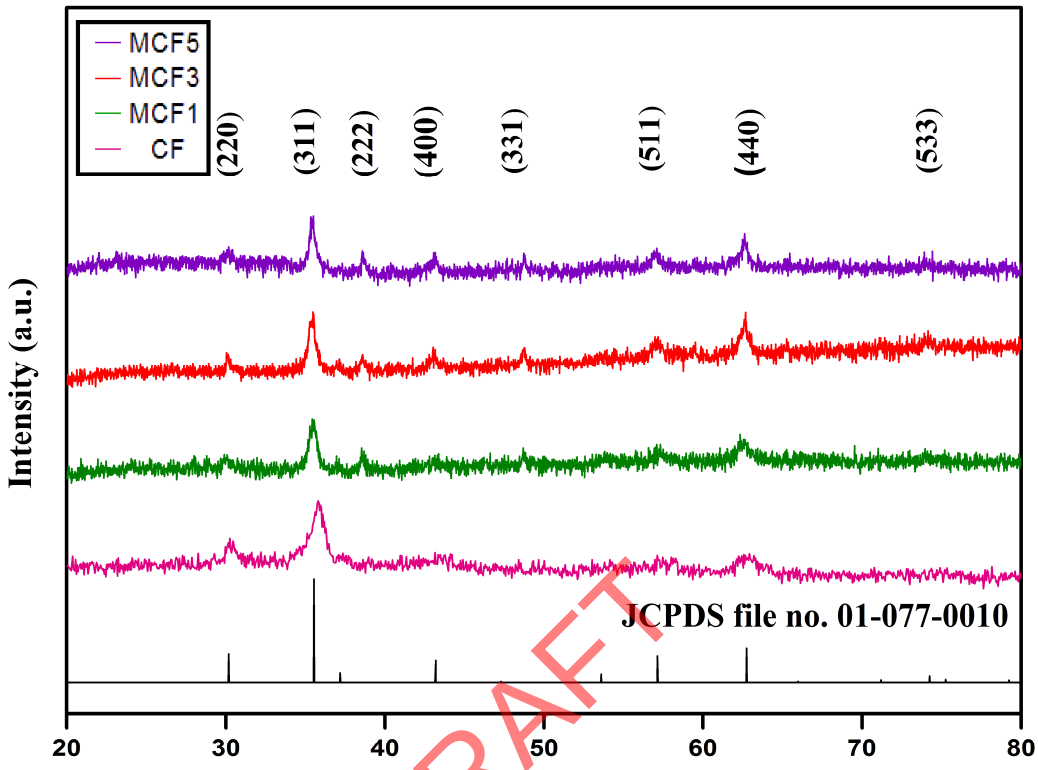

Figure 1. XRD spectra of bare and MCFs nanoparticle.

Figure 1 shows the XRD profiles of CF and MCFs nanoparticles. The principal (Maximum intensity) X-ray diffracted peaks observed from (220), (311),(222), (400), (331), (511), (440) and (533) planes at diffracted glancing angles 30.30°, 35.78°,37.18°, 43.30°, 47.30°, 57.27°,62.72° and 74.24°, respectively are associated to the cubic crystal structure with the space group of Fd-3m. Moreover, these values exactly match with the JCPDS file no. 01-077-0010. With the help of Debye-Scherrer formula and in association with Lorentz fit method, the average size of the above nano-crystallite was found to be 8.81 nm, 13.38 nm 15.35 nm and 18.69 nm from full width half maximum of (311) plane for CF, MCF1, MCF3 and MCF5, respectively and they showed the nanostructure characteristics. The predominant peaks from (311) planes observed at 35.78°, 35.47°, 35.43° and 35.41° for CF, MCF1, MCF3 and MCF5, respectively indicate the increase in lattice constant based on Bragg's diffraction law. As the size is in the order of nano, it would help the ions (OH^-) to diffuse in the electrolyte, consequently, higher values of capacitances could be achieved.

3.2. Elemental Analysis of CF and MCFs electrodes:

In order to evaluate the percentage of elemental compositions present in the synthesized nanoparticles of CF and MCF samples, Energy Dispersive X-ray (EDX) study was performed and the presence of O, Fe, Cu and Mg elements in the synthesized samples was confirmed. Moreover, the percentages of Mg and Cu obtained from EDX profile of CF and MCFs have been in line well with the desired amount of Mg and Cu based on stoichiometric calculations and the data have been given in Table I. From Table I, it can be noted that the physical surrounding namely ambient temperature, ambient pressure and humidity conditions are in favor of synthesizing the nanoparticles of CF and MCFs with the required stoichiometry.

Table I. The arrived and expected weight and atomic percentage of elements in CF and MCFs

S. No.	Composites	Percentage	OK	FeK	CuK	MgK	Total
1	CF	Wt. % (A)	28.81	45.53	25.66	00.00	100.00
		Wt. % (E)	26.74	46.69	26.57	00.00	100.00
		At. % (A)	59.64	26.99	13.37	00.00	100.00
		At. % (E)	57.14	28.57	14.29	00.00	100.00
2	MCF1	Wt. % (A)	21.20	55.85	21.95	01.01	100.00
		Wt. % (E)	27.20	47.50	24.30	01.00	100.00
		At. % (A)	48.86	36.88	12.71	01.53	100.00
		At. % (E)	57.14	28.57	12.86	01.43	100.00
3	MCF3	Wt. % (A)	20.51	60.23	14.99	04.27	100.00
		Wt. % (E)	28.10	46.10	19.60	03.20	100.00
		At. % (A)	46.25	38.91	08.51	06.33	100.00
		At. % (E)	57.15	28.57	09.99	04.29	100.00
4	MCF5	Wt. % (A)	27.21	49.91	13.95	08.94	100.00
		Wt. % (E)	29.13	50.87	14.47	05.53	100.00
		At. % (A)	53.45	28.09	06.90	11.56	100.00
		At. % (E)	57.15	28.57	07.14	07.14	100.00

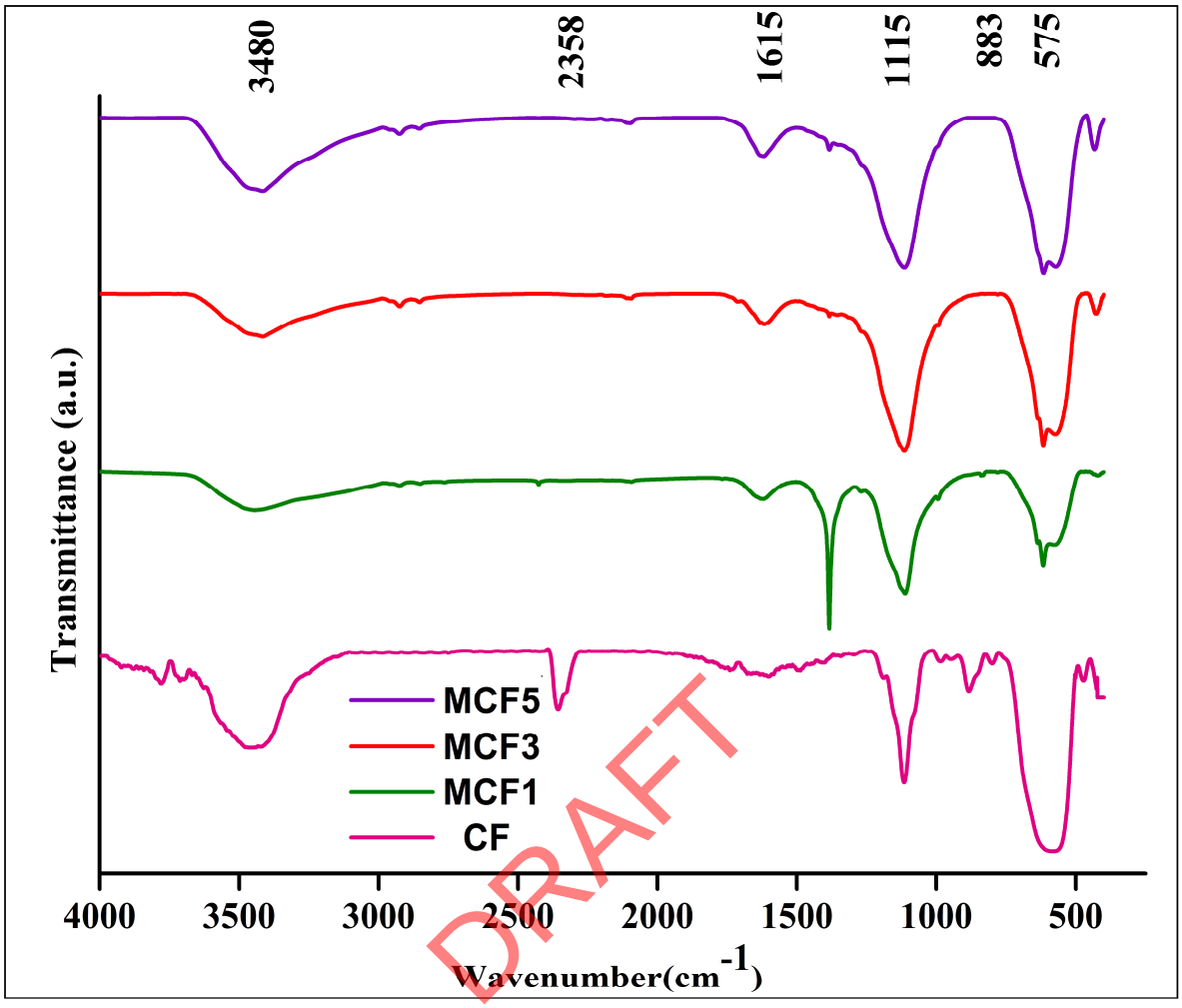

Figure 3 – FT-IR spectra of bare CF and MCF samples

For the purpose of detecting the functional groups available in the synthesized nanocomposites of CF and MCFs, FT-IR spectra examination was carried out. The FT-IR spectral profiles of bare CF and MCFs nanoparticles scanned in the range 4000 to 500 cm^{-1} at room temperature are shown in Figure 3. The stretching vibrations of tetrahedral sites of Fe^{3+}– O^{2-} is observed at 575 cm^{-1}. The very weak band at 883 cm^{-1} points out the formation of the spinel phase of copper ferrite associated as a result of vibration between Cu and O atoms. The band at 1115 cm^{-1} is caused as a result of some residual water molecule in the sample during the synthesis of the nanoparticle. Band δ (OH) is occurred at 1384 cm^{-1} due to presence of H_2O molecule in MCF1 [17]. The intensity of the peak is found to be reduced at higher concentration of Mg.

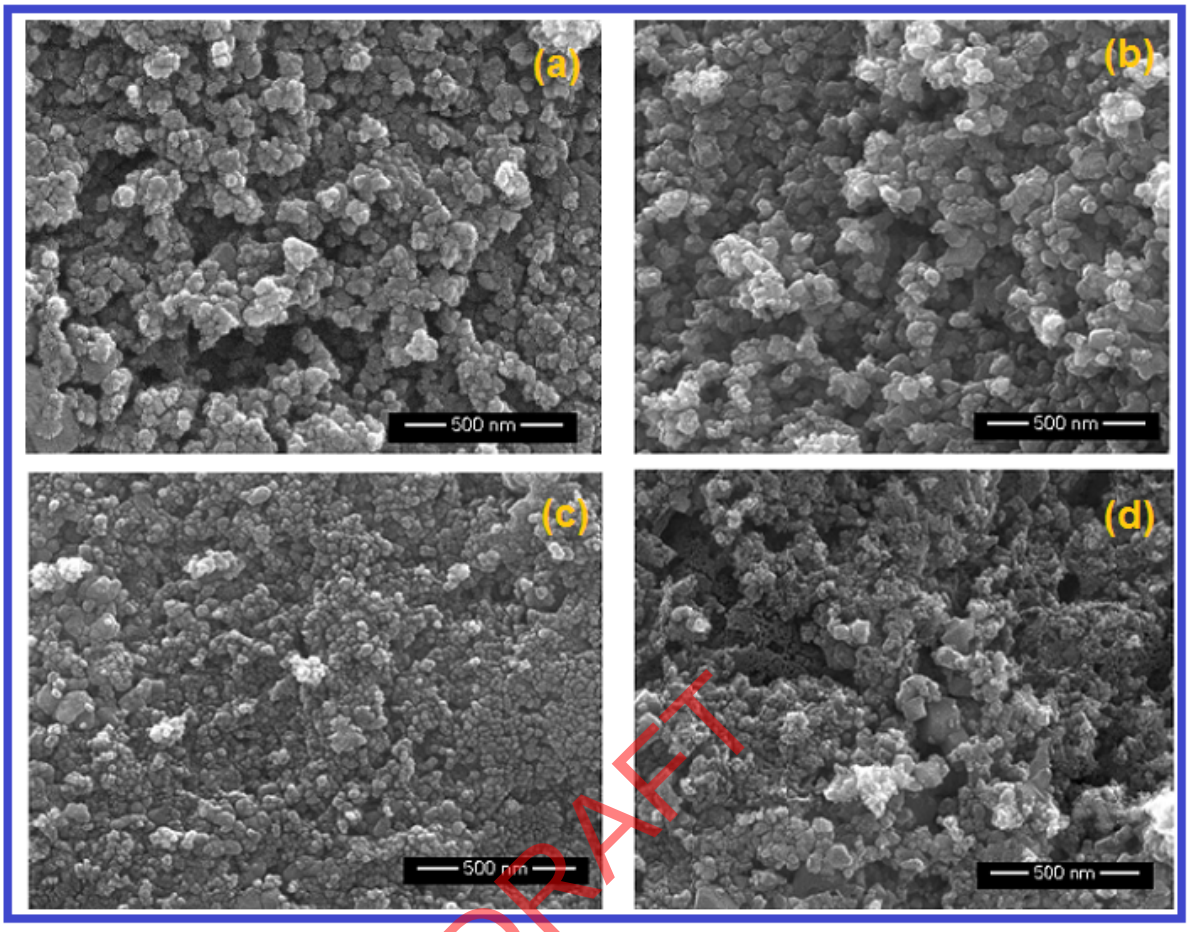

Figure 4. SEM images of (a) bare CF (b) MCF1, (c) MCF3 and (d) MCF5 at 500 nm scale

In order to choose the electrode materials for making supercapacitor, the nanomaterial's surface morphology plays a significant role since the transportation of charge carriers take place through surface. Hence High-Resolution Scanning Electron Microscopy (HRSEM) examination was performed to explore the surface morphology of $Cu_xMg_{1-x}Fe_2O_4$ (x=1, 0.9, 0.7 and 0.5) nanoparticles and the images are shown in Figure 4. They were proven to be homogeneous and agglomerated nanoparticles of CF and MCFs. From these images, it could be ascertained that the average size of the particle of CF and MCFs would be in the order of nanometer by the assembly of sub micrometric particles. The texture and porosity of MCF3 nanoparticles indicate that the sample is the desirable candidate for making electrode for supercapacitors.

3.3 Electrochemical Analysis of CF and MCFs electrodes:

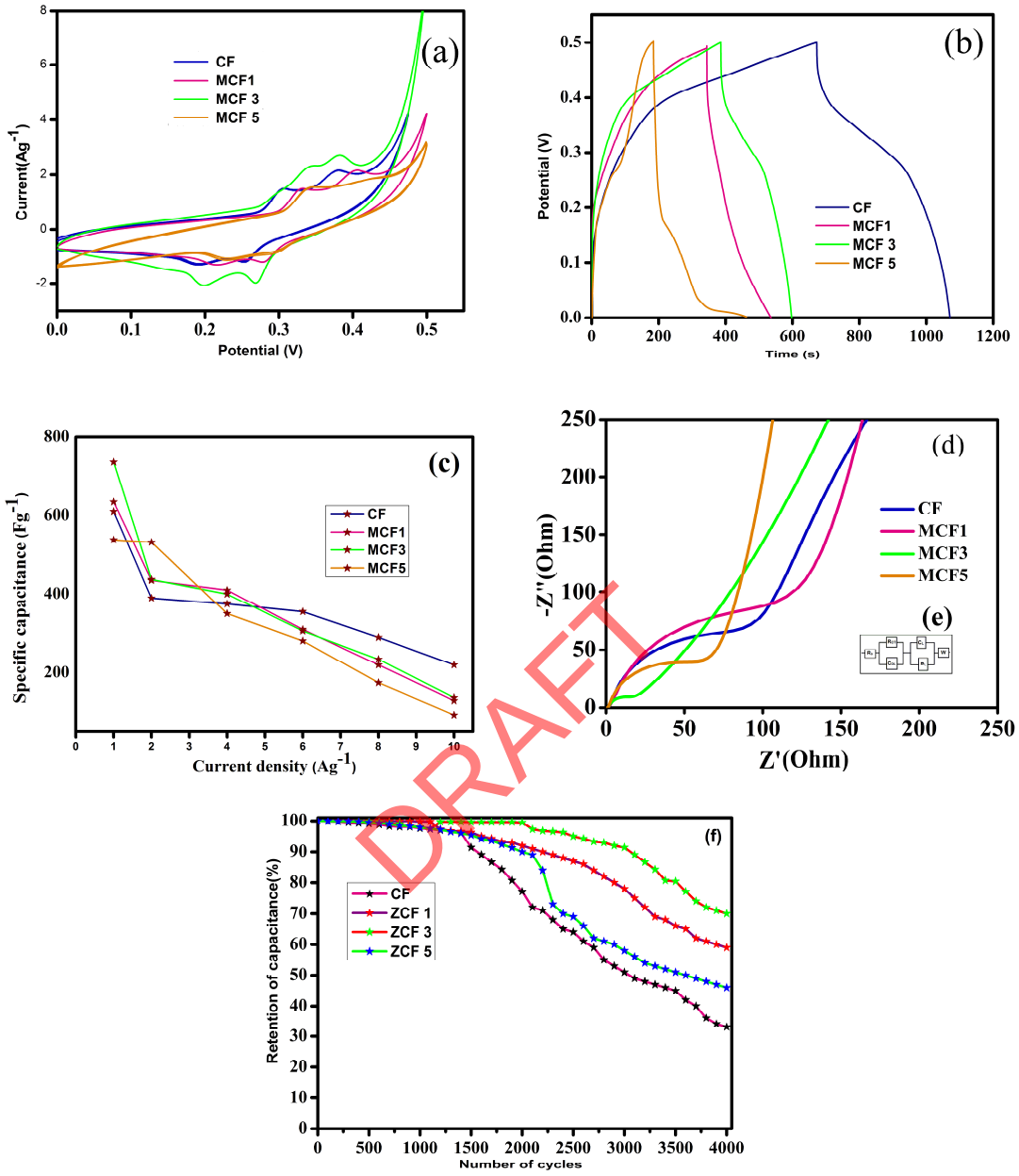

Figure 5 (a) CV curves of CF and MCF electrodes at a scan rate of 5 mV s^{-1}, (b) GCD profiles of CF and MCF electrodes at a current rate of 1 A g^{-1}, (c) Variation of capacitance at different current densities, (d) Nyquist plot for CF and MCF electrodes (inset (e) modified Randles circuit model) and (f) Cyclic stability plot for CF and MCF electrodes

With the aid of conventional three-electrode cell arrangement, the electrochemical performances of CF and MCFs electrodes were examined using CV and galvanostatic charge-discharge (GCD) curve in the potential aperture between 0 and 0.5 mV s^{-1} in 2 M KOH electrolyte

and the results are illustrated in Figure 5 in which (a) illustrates the CV curves of CF, MCF1, MCF3, and MCF5 electrodes at the voltage sweep rate of 5 mV s^{-1}. Initially, the CV measurements were carried out at a different potential scan rate of 2, 5, 10, 25, 50, 75 and 100 mV s^{-1} to analyze the nature of the energy storage mechanism CF and MCF electrodes.

These observed CV curves suggest that charge storage and discharge processes could be attributed to the faradaic nature due to presence of well-defined oxidation and reduction peaks. Since the faradaic reaction includes the transfer of two electrons, there is a large area under the CV curve, due to the quasi-conversion reaction mechanism. The degree of the anodic and cathodic current is comparable showing that the charge storage performance is even, and there is a comprehensive conversion of Cu to CuO (Cu^0 - Cu^{2+}) during the oxidation and vice versa (Cu^{2+} - Cu^0) in reduction process. In forward scan, i.e., during the anodic current, electrode is oxidized by emitting the electron, unbalancing charges leaving the material, corresponding to the anodic peak (Cu^0 - Cu^{2+}) at a potential ranging from 300 to 400 mV for all scan rates. The process is retreated in the case of the reduction process during reverse scan i.e., the cathodic current and the cathodic peak (Cu^{2+} - Cu^0) is seen at around 200 mV for all scan rates. This observation indicates that CF and MCF nanoparticle electrodes are probable to be electrode materials for making the supercapacitor. Further, a larger area under the CV curve with the increasing scan rate indicates that the electrodes of CF/MCF display a great rate of capability of electron discharge. There is a large area under the CV curve, which accounts for the quasi-conversion reaction mechanism. This indicated that MCF3 has enhanced the electrochemical activity and specific capacitance attributable to the electrochemically active Mg^{2+} ions in the samples that reduce the internal resistance. The specific capacities of the electrodes are estimated to be 620, 635, 737.5 and 537.5 F g^{-1} for CF, MCF1, MCF3 and MCF5, respectively, using the area under the CV curve. Larger specific capacitance values account for electrolyte ions (OH^- ions) in the electrolyte have enough time to react the active sites of the electrodes made up of CF and MCFs at lower current contour and OH^- ions are migrated from the KOH electrolyte solution into the composite electrodes in order to maintain charge neutrality. These results are pretty comparable with the values reported by other research groups.

The charging and discharging characteristics of the CF and MCFs electrodes were observed with the galvanostatic charge–discharge cyclic examination. In order to analyze the charge storage ability of $Cu_xMg_{1-x}Fe_2O_4$ (x=1, 0.9, 0.7, and 0.5) samples, the GCD measurements were performed.

The GCD profiles of CF, MCFs samples at a current density of 1 A g^{-1} between the potential window between 0 and 0.5 V are presented in Figure 5 (b). The capacitive behavior is predominantly influenced by current density and IR drop to some extent.

With the aim of study of collective behaviour of both resistive and capacitive properties of CF and MCFs electrodes materials, electrochemical impedance spectra (EIS) examination was executed. The Figure 5 (c) represents the Nyquist impedance graph in the frequency range 0 to 250 kHz at open circuit voltage of 5 mV with standard 3 electrode configuration. A Modified Randles circuit model is presented in Figure 5 (d) as inset in Figure 5 (c), in which R_{CT} represents charge transfer resistance, C_L is the mass capacitance, D_{DL} is the double layer capacitance and W is the Warburg element, respectively. There are two different contours in the impedance spectra namely a semicircle arc in the high frequency zone referred as the knee frequency and a straight line at the lower frequency region denoting the Warburg impedance. A comprehensive results of solution resistance (R_s) is owing to ions in the electrolytic, inherent active material and the contact between electroactive material and current accumulator interface, which is established from the high frequency range of Nyquist plot marked by the intercept at real part (Z') on the X- axis whose values were found to be 86 Ω, 107 Ω, 27 Ω, and 69 Ω, for CF, MCF1, MCF3 and MCF5, respectively. At higher frequency zone, the semicircle arc emphasises the charge-transfer resistance (R_{CT}) building attributed to the Faradaic reactions in the nanocomposite material and double-layer capacitance on the surface electrodes. The (R_{CT}) of the MCF3 (27 Ω) and CF (56 Ω) clearly indicates a 50% improvement due to the presence of magnesium. The smaller R_{CT} of magnesium copper ferrite nanocomposites show improved conductivity through charge-discharge phenomena at higher current densities of MCF electrodes.

The specific capacitance profiles of MCFs and CF electrodes in a 2 M KOH electrolyte at various current densities (1 to 10 Ag^{-1}) are shown in Figure 5 (e). At the lowest current density of 1 A g^{-1}, the highest specific capacitance was estimated to be 737.5 F g^{-1} for MCF3 among all the electrodes which shrunk when go for higher current densities. IR drop could be the one of the reasons because part of voltage is used to cross the IR drop barrier and the remaining voltage is utilized to charge the supercapacitor made up of CF/MCF nanoparticles. Hence, the active voltage (ΔV) aperture will be dwindled. The IR drop is inevitable because it arises due to comprehensive resistances offered by electrodes made up of CF/MCFs, liquid electrolyte (2 M KOH) and metal contact resistances created in three-electrode cell configuration. The IR drop of CF, MCF1, MCF3,

and MCF5 are 3.05, 2.7, 1.07, and 2.69Ω, respectively. There is a pretty loss of electrical energy owing to IR drop that would be significant at greater current density, due to usage of repeated number of cycles including both charging and discharging known as aging. It is motivating that MCF3 electrode retains 70% of specific capacitance value (737.5 F g^{-1}) at a current density of 1 A g^{-1} up to 4000 cycles whereas CF electrode quickly diminishes and retains only 33% of initial capacitance value (620 F g^{-1}). This is due to the inclusion of Mg in the nano-composite electrode, which creates relatively better active sites on the surface of the electrode.

M. Mayakkannan et al. synthesized ternary transition metal ferrite ($NiCoFe_2O_4$) and reported the maximum specific capacitance value of 314.97 F g^{-1} at the scan rate of 5 mV s^{-1} [18]. Gayathri Manju et al. prepared nickel–copper mixed ferrite nanoparticles [$Cu_{1-x}Ni_xFe_2O_4$ (x = 0, 0.5, 1)] nanoparticles by combustion method and stated the specific capacitance of 114 F g^{-1} which was obtained at the scan rate of 5 mV s^{-1} for the same using a three-electrode system in 1 M KOH electrolyte solution [19]. B. Saravanakumar et al. obtained the spherical monodispersed $CuFe_2O_4$ nanoparticles adopting facile solvothermal route and stated the specific capacitance of BS1 is 189.2 F/g at current density 0.5 A/g using 1 M of KOH solution [20]. X. Wu et al. found that the $CuFe_2O_4$ sample at 400° C could deliver a reversible specific capacity of 281 mA h g^{-1} at a current density of 100 mA g^{-1} after 20th cycles [21]. Rongyue Wang et al. prepared $MnFe_2O_4$ colloidal nanocrystal clusters for electrode materials that showed specific capacitance values of 97.1, 93.9,74.2 and 47.4 F g^{-1} in various 2 M electrolytes namely KOH, NaOH, LiOH and Na_2SO_4, respectively [22]. Dewei Wang et al. obtained Fe_2O_3–graphene nanocomposite which exhibits large specific capacitance value of 151.8 F g^{-1} at 1 A g^{-1} [23]. Min Fu et at. made an electrode with the help of nickel ferrites/graphene composites which exhibited a specific capacity of 481.3 F g^{-1} at a current density of 0.1A g^{-1}, and 298.2 F g^{-1} at 10 A g^{-1} in 6 M aqueous KOH solution [24]. V.S. Kumbhar et al. formed a cobalt ferrite thin film on stainless steel substrate *via* simple chemical route and it shows the maximum specific capacitance value of 366 F g^{-1} in 1 M NaOH aquaous alkaline solutions at the scan rate of 5 mV s^{-1}[25]. K. Sathiyamurthy et al prepared $Co_xZn_{1-x}Fe_2O_4$ with varying concentrations of zinc ferrite (x = 0.0, 0.5, 1.0), cobalt-doped zinc ferrite, and cobalt ferrite NPs by a simple co-precipitation route. There was an obviously improved specific capacitance of 218 Fg-1 in $Co_{0.5}Zn_{0.5}Fe_2O_4$ at the scan rate of 10mV/s [26].

In general, electrochemical analysis with a conservative two-electrode setup is more reliable for testing the desirability of the prepared nanocomposite for commercial applications of supercapacitors. In this view, in order to study the electrochemical activities of the nanocomposite electrode, as shown in Figure 6, a two-electrode configuration with MCF3 and high surface AC, polypropylene used as bifurcated sheet in a 2 M KOH electrolyte with an asymmetric type of SC device was fabricated on an electrochemical workstation . Figure 7 (a) exhibits the CV curves of MCF3//AC asymmetric type device at different voltage sweep rates between 10 and 100 mV s^{-1} in the potential window from 0 V to 1.4 V. Better repeatability, reversibility and good capacitive behaviour of the device which account for a kind of quasi-rectangular shape of the curves could be observed and found to be retained at all scan rates from the CV graph profile of SC cell. GCD is better to estimate the capacitance value of a supercapacitor between CV and GCD, since the quantum of energy stored is quantified with the runtime of the experiment in GCD, whereas, the analysis time is governed by the rate at which the scanning takes place and the width of the potential window in CV. Figure 7 (b) depicts the GCD measurements carried out for this device at different current densities from 2 to 10 A g^{-1} with an increasing order of 2 A g^{-1}. These values confirm the electrochemical performance through the faradaic process. The maximum specific capacitance asymmetric type supercapacitor device was measured to be 230 F g^{-1} for MCF3//AC device at 2 A g^{-1}, where the specific capacity of was estimated by calculating the area of the GCD curve. The estimated specific capacitances of MCF3//AC asymmetric type device are 230, 148, 79, 52 and 29 at current densities of 2, 4, 6, 8, and 10 A g^{-1}, respectively, as shown in Figure 7 (c). MCF3//AC device is examined in order to check the cyclic stability by charging and discharging test (depicted in Fig. 7 (d)). It was found to be 76% up to 4000 cycles at a current rate of 10 A g^{-1} that governs its overall performance.

Table. II. Electrochemical performance of MCF3//AC asymmetric stype supercapacitor

S.No.	Current density	Specific capacitance	Energy density	Power density
Unit	A g^{-1}	F g^{-1}	W h kg^{-1}	W kg^{-1}
1	2	230.0	62.61	1168
2	4	147.6	40.18	2333
3	6	78.5	21.23	3474
4	8	52.4	14.26	4667
5	10	29.8	8.11	5839

The Nyquist plot of MCF3//AC asymmetric type of SC is presented in Figure 7 (e). The charge transfer resistance (R_{CT}) value of MCF3//AC device is 41 Ω, as a result of addition of activated carbon. Since a minor resistance is added to the device, the R_{CT} value of MCF3//AC is convincingly greater than the R_{CT} values estimated in three-electrode cell setup. The Ragone plot for MCF3//AC device is shown in Figure 7 (f). The maximum estimated energy density and power density of MCF3//AC device on the basis of GCD investigation are 62.61 W h kg^{-1} and 1167 W kg^{-1}, respectively, which was convincingly higher than a previous report. Ankur Soam et al. observed maximum energy density and power density for ferrite and graphene composite supercapacitor as 5.5 Wh/kg with power density of 900 W kg^{-1} using 1 M Na_2SO_4 electrolyte at room temperature [27]. Yuqi Jiang et al. reported a novel flexible asymmetric supercapacitor made of CVD-grown nickel nanoparticle@carbon nanotube (Ni@CNT) network films that delivered high volumetric energy density of 1.39 mWh cm^{-3} and power density of 440 mW cm^{-3}, as well as excellent cycleability up to 10,000 times [28]. Safa Polat et al. prepared $CuFe_2O_4$ together with g-C_3N_4 and GNPs in various combinations and reported the energy and power densities as 27.8 mWh/cm^2 and 300 mW/cm^2 respectively [29]. Shubra Lalwani et al. fabricated a cell with nanorods as a positive electrode in asymmetric configuration, whereas graphene nanoribbons as negative electrode which exhibits an outstanding energy density of 33.5 W h kg^{-1} at 727.8 W kg^{-1} [30]. K. Vijaya Sankar et al. fabricated rGO based hybrid supercapacitor ($CoFe_2O_4$//rGO) that provides a good specific capacitance 38 F g^{-1} and energy density 12.14 W h kg^{-1} at 3 mA with good cycle life [31]. Z. Song et al. synthesized magnesium-doped nickel-based (BMDNB) electrode material successfully on a foamed nickel substrate by one-step hydrothermal method and achieved a maximum energy density of 74.9 W h kg^{-1} at a power density of 1086.8 W kg^{-1} [32]. The inclusion of magnesium in the copper ferrite nano-composite elevates the electrochemical features like specific capacitance, energy density and power density of the asymmetric type supercapacitor when compared with bare copper ferrites. This is due to formation of auxiliary active sites for ion diffusion in electrolyte, synergistic effects between electrode and electrolyte which in turn results in an enhanced supercapacitor with better endurance limit, energy density and power density. The present investigation proposes that magnesium-doped copper ferrite electrodes can be explored to devise high performance supercapacitors.

In the present study, various concentrations of Mg, were used as dopants to synthesize metal-doped copper ferrites. The nanocomposites were employed as electrodes and their supercapacitive features have been thoroughly investigated. In future the work can be extended with other potential dopants to improve the electrochemical performance of asymmetric supercapacitors. Also, the effect of multi-metal doping can be explored, which may contribute to the understanding of mechanism of supercapacitive behaviour of novel materials. As far as commercialization is concerned, cost-effective materials and methods are essential. In this regard, electrodes with low-cost metal oxides with superior electrochemical properties can be employed in the fabrication of supercapacitors. Further, in an eco-friendly point of view these materials can be synthesized by greener methods. Innovative nanostructures such as double walled and triple walled hallow spheres are highly favourable for achieving high performance. With respect to the cell configuration, stable electrolytes with broad cell voltage may be used to fabricate advanced supercapacitor devices. Similarly, traditional electrolytes may be replaced with ionic liquid electrolytes possessing wide cell voltage may be employed to enhance the performance. Novel methods may be developed to control precisely the morphology of electrode materials as it is another aspect to improve capacitance in supercapacitors. Thus, revolutionary breakthroughs on the configuration of supercapacitors will make new pathways in the fields of automobiles especially electric vehicles, robotics, cameras, backup power system, renewable and sustainable energy devices, wearable and self-healing supercapacitors, and biotechnology.

In the present work, we have used the homogeneous solution of 100 mL for the microwave combustion process in the microwave system (800 W, CE1041DFB/XTL, and 2.54 GHz frequency) for 10 minutes. It is found in the literature that the microwave systems of 1.2 MW is commercially available which could speed up the combustion process and thereby reduce the combustion time to few minutes. Also, these microwave sytems could be able to hold a capacity of 1.5 L of homogeneous solution for microwave combustion process. This speedy combustion process together with large holding capacity of the homogeneous solution could benefit the large scale production of nanomaterials for making electrode materials to supercapacitors. However, optimizing the annealing temperature and time could be a challenge at the initial phase for large scale production of the materials.

Conclusions

In summary, pure and Mg-doped copper ferrite nanoparticles have been synthesized *via* quick, reliable and facile microwave combustion route. Crystal structure and surface morphological studies have been conducted through XRD and SEM that reveals the successful synthesis of $Cu_xMg_{1-x}Fe_2O_4$ (x=1, 0.9, 0.7, 0.5) nanoparticles. The electrochemical studies reveal that inclusion of magnesium increases the electrochemical features and the maximum specific capacitance value of $Cu_{0.7}Mg_{0.3}Fe_2O_4$ have been found to be 437.5 F $g^{-1}$with good charging and discharging stability. The MCF3//AC supercapacitor exhibits the delivery of maximum energy density and power density as 62.61 W h kg^{-1} and 1168 W kg^{-1}, respectively, at the current density of 2 A g^{-1}. We consider that our synthesized magnesium-doped copper ferrite nanocomposite could be a promising electrode candidate for high power supercapacitor applications.

Ethical approval

I am the corresponding author and I declare that the manuscript should not be submitted to more than one journal for simultaneous consideration. The authors agree to publish the manuscript in the Journal of Electronic Materials

Financial Competitive

The authors declare no competing financial interest.

Research Data Policy and Data Availability Statements

The data generated during the current study are available from the corresponding author on reasonable request.

Author Contribution

All author contribute equally to this work

M. Selvakumar contributes to conceptualization, methodology and synthesis of Nanoparticles

S. Maruthamuthu contributes to coin the problem and frame of workflow, formal analysis

E. Vijayakumar contributes to conceptualization, data collection and reviewing of workflow

B. Saravanakumar contributes to interpretation of data

A. Tony Dhiwahar contributes to draft writing and reviewing and editing the manuscript

Conflict of interest

The authors declare that they have no conflicts of interest

References

[1] J Zhang and X. Wu, Dual-ion carrier storage through Mg^{2+} addition for high-energy and long-life zinc-ion hybrid capacitor. Int. J. Miner. Metall. Mater. 31,179 (2024).

[2] H Liu, M Dai, D Zhao, X Wu, B Wang, Realizing Superior Electrochemical Performance of Asymmetric Capacitors through Tailoring Electrode Architectures. ACS Appl. Energy Mater. 3, 7004 (2020).

[3] X Wang, Y Sun, W Zhang and X Wu, Flexible $CuCo_2O_4$@Ni-Co-S hybrids as electrode materials for high-performance energy storage devices, j.cclet.34, 107593 (2023).

[4] J Liu, S Zhao, A Umar, X Wu, Constructing high-capacitance electrochemical capacitors through the introduction of V ions into MoS_2/Ni_3S_2 nanosheets. Materials Today Sustainability. 23, 100433 (2023).

[5] D. Alhashmialameer, S. Ullah, A. Irshad, I.A. Alsafari, H.H. Abd El-Gawad, M.A. Abdelrahman Elsheikh, X. Liu, and S. Bashir. Copper-doped magnesium ferrite and its composite with rGO: Synthesis, characterization, and degradation of organic effluents and antibacterial study. Ceram. Int.48, 24100 (2022).

[6] Tian Liu, Linsheng Wang, Ping Yang and Bingyuan Hu, Preparation of nanometer $CuFe_2O_4$ by auto-combustion and its catalytic activity on the thermal decomposition of ammonium Perchlorate. Mater. Lett. 62, 4056, (2008).

[7] Monika Saini, S. K. Singh, Rajni Shukla and Ashok Kumar, Mg Doped Copper Ferrite with Polyaniline Matrix Core–Shell Ternary Nanocomposite for Electromagnetic Interference Shielding. J. Inorg. Organomet Polym. Mater. 28, 2306 (2018).

[8] M. Abdullah Dar Vivek Verma S.P.Gairola W.A. Siddiqui Rakesh Kumar Singh R.K.Kotnala,Low dielectric loss of Mg doped Ni-Cu-Zn nano-ferrites for power applications. Appl. Surf. Sci. 258, 5342 (2012).

[9] M.A. Ahmed, H.H. AfifyI.K.El, Zawawia and A.A. Azab, Novel structural and magnetic properties of Mg doped copper nanoferrites prepared by conventional and wet methods. J. Magn. Magn Mater. 324, 2199 (2012).

[10] M.A. Gabal, Effect of Mg substitution on the magnetic properties of NiCuZn ferrite nanoparticles prepared through a novel method using egg white. J. Magn. Magn Mater. 321, 3144 (2009).

[11]Yuan Zhou, Wen Chen, Yuexiao Shen, Xuehang Wu, Wenwei Wu and Juan Wu, Lattice strains and magnetic properties evolution of copper-magnesium ferrite with lithium substitution. J. Magn. Magn Mater. 396, 198 (2015).

[12] Unchista Wongpratat, Pannawit Tipsawat, Jessada Khajonrit, Ekaphan Swatsitangand Santi Maensiri, Effect of Nickel and Magnesium on electrochemical performances of partial substitution in spinel ferrite. J. Alloys Compd. 831,154718 (2020).

[13] M.K. Shobana, Kyungbae Kim, Jae-Hun Kim, Impact of Magnesium substitution in Nickel ferrite: Optical and Electrochemical studies. Physica E Low Dimens. Syst. Nanostruct. 108, 100 (2019).

[14] Manpreet Kaur, ShwetaRanaand P.S.Tarsikka, Comparative analysis of cadmium doped magnesium ferrite $Mg_{(1-x)}Cd_xFe_2O_4$ (x=0.0, 0.2, 0.4, 0.6) nanoparticles. Ceram Int. 38, 4319 (2012).

[15] H.M. Zaki, S Al-Heniti, and T.A. Elmosalami, Structural, magnetic and dielectric studies of copper substituted nano-crystalline spinel magnesium zinc ferrite. J.Alloys Compd. 633, 104 (2015).

[16] N. Valaralxmi and K.V. Sivakumar, Structural and dielectric studies of magnesium substituted NiCuZn ferrites for microinductor applications. Mater Sci Eng. B. 184, 88 (2014).

[17] Z. Mitic, G.S. Nikolic, M. Cakic, P. Premovic, L. Ilic, FTIR spectroscopic characterization of Cu(II) coordination compounds with exopolysaccharide pullulan and its derivatives. j.molstruc.924, 264 (2009).

[18] M.Mayakkannan, A.Murugan, A.Shameem, V.Siva, S.SasikumarS.Thangarasu S. AsathBahadu Investigations on ternary transition metal ferrite: NiCoFe2O4 as potential electrode for supercapacitor prepared by microwave irradiation method. J.Energy Storage. 44 103257(2021).

[19] B. GayathriManju and P. Raj, Green Synthesis of Nickel–Copper Mixed Ferrite Nanoparticles: Structural, Optical, Magnetic, Electrochemical and Antibacterial Studies.J. Electron. Mater. 78, 7710 (2019).

[20] B. Saravanakumar, S.P.Ramacahndran, G. Ravi, V. Ganesh, Ramesh K. Guduru and R. Yuvakkumar, Electrochemical performances of monodispersed spherical $CuFe_2O_4$ nanoparticles for pseudocapacitive applications.Vacuum. 168, 108798(2019).

[21] Xuehang Wu, Wenwei Wu, Yongni Li, Feng Li and Sen Liao, Synthesis and electrochemical performance of rod-like $CuFe_2O_4$ as an anode material for Na-ion battery. Mater.lett. 138, 192 (2015).

[22] Rongyue Wang, Qun Li, ulu Cheng, Hongliang Li, Baoyan Wang, X.S.Zhao and PeizhiGuo,Electrochemical properties of manganese ferrite-based supercapacitors in aqueous electrolyte: The effect of ionic radius. Colloids Surf. A: Physicochem Eng. Asp. 457, 94-99 (2014).

[23] Dewei Wang, Yuqi Li, Qihua Wang and Tingmei Wang, Nanostructured Fe_2O_3–graphene composite as a novel electrode material for supercapacitors. J. Solid state Chem. 6, 2095(2012).

[24] Min Fu, Wei Chen, Xixi Zhu and Qingyun Liu, One-step preparation of one dimensional nickel ferrites/graphene composites for supercapacitor electrode with excellent cycling stability.J. Power Sources. 96, 41 (2018).

[25] V.S.Kumbhar, A.D.JagadaleN.M.Shinde and C.D.Lokhande, Chemical synthesis of spinel cobalt ferrite ($CoFe_2O_4$) nano-flakes for supercapacitor application. Appl.Surf. Sci. 259, 39 (2012).

[26] K. Sathiyamurthy, C. Rajeevgandhi , L. Guganathan, S. Bharanidharan, and S. Savithiri, Enhancement of magnetic, supercapacitor applications and theoretical approach on cobalt-doped zinc ferrite nanocomposite. J.Mater. sci: Mater. Electron. 32, 11593(2021).

[27] Ankur Soam, Rahul Kumar,vDhirendranath Thatoi1 and Mamraj Singh, Electrochemical Performance and Working Voltage Optimization of Nickel Ferrite/Graphene Composite based Supercapacitor.J.Inorg.Organomet. Polym.Mater. 30, 3325 (2020).

[28]Yuqi Jiang, Cheng Zhou and Jinping Liua, A non-polarity flexible asymmetric supercapacitor with nickel nanoparticle@carbon nanotube three-dimensional network electrodes. Energy storage materials. 11, 75 (2018).

[29] Safa polat and Dana Faris, Fabrication of $CuFe_2O_4$@g-C_3N_4@GNPs nanocomposites as anode material for supercapacitor applications.Ceram. Int. 48. 24609 (2022).

[30] Shubra Lalwani, Ram BhagatMarichi ,Monu Mishra, Govind Gupta, GurmeetSingh and Raj Kishore Sharma, Edge enriched cobalt ferrite nanorods for symmetric/asymmetric supercapacitive charge storage. Electrochimi.Acta. 283, 708 (2018).

[31] K. VijayaSankar, R. KalaiSelvan and Danielle Meyrick, Electrochemical performances of CoFe2O4 nanoparticles and arGObased asymmetric supercapacitor. RSC Adv. 5, 99959, (2015).

[32]Zeyu Song, Jihuai Wu, Guodong Li, Xiaobing Wang, Tingting Zhu, Chenglong Geng, Na Liu, Leqing Fan, Jianming Lin, Basic magnesium-doped nickel-based electrodes with card-on-lawn structure for supercapacitor with high energy density. j.jelechem. 863, 114040 (2020).